

# ESTIMATION OF NORMALIZED COHERENCY MATRIX THROUGH THE SIRV MODEL. APPLICATION TO HIGH RESOLUTION POLSAR DATA

G. Vasile<sup>(1)</sup>, J.-P. Ovarlez<sup>(2),(3)</sup>, F. Pascal<sup>(3)</sup>, and M. Gay<sup>(1)</sup>

<sup>(1)</sup>GIPSA-lab, CNRS - Grenoble INP, 961 rue de la Houille Blanche, BP 46, 38402 Grenoble Cedex, FRANCE  
Email: {gabriel.vasile|michel.gay}@gipsa-lab.inpg.fr

<sup>(2)</sup>French Aerospace Lab, ONERA DEMR/TSI - Chemin de la Huniere, 91761 Palaiseau Cedex, FRANCE  
Email: ovarlez@onera.fr

<sup>(3)</sup>SONDRA, Supélec - Plateau du Moulon, 3 rue Joliot-Curie, 91192 Gif-sur-Yvette Cedex, FRANCE  
Email: frederic.pascal@supelec.fr

## ABSTRACT

In the context of non-Gaussian polarimetric clutter models, this paper presents an application of the recent advances in the field of Spherically Invariant Random Vectors (SIRV) modelling for coherency matrix estimation in heterogeneous clutter. The complete description of the POLSAR data set is achieved by estimating the span and the normalized coherency independently. The normalized coherency describes the polarimetric diversity, while the span indicates the total received power. The main advantages of the proposed Fixed Point estimator are that it does not require any "a priori" information about the probability density function of the texture (or span) and it can be directly applied on adaptive neighbourhoods. Interesting results are obtained when coupling this Fixed Point estimator with an adaptive spatial support based on the scalar span information. Based on the SIRV model, a new maximum likelihood distance measure is introduced for unsupervised POLSAR classification. The proposed method is tested with airborne POLSAR images provided by the RAMSES system. Results of entropy/alpha/anisotropy decomposition, followed by unsupervised classification, allow discussing the use of the normalized coherency and the span as two separate descriptors of POLSAR data sets.

Key words: non-Gaussian clutter; POLSAR; estimation; segmentation; high resolution.

## 1. INTRODUCTION

A Synthetic Aperture Radar (SAR) measures both amplitude and phase of the backscattered signal, producing one complex image for each recording. The sensors being able to emit or receive two orthogonal polarizations, fully POLarimetric Synthetic Aperture Radar (POLSAR) systems describe the interactions between the electromagnetic wave and the target area by means of the Sinclair

matrix [1]. The polarimetric diversity can be employed for investigating various physical properties of the studied media. The recent availability of spaceborne POLSAR imagery from ALOS and RADARSAT-2 satellites has resulted in increased interest in ground cover classification and monitoring, such as forests, snow, ice, agricultural or urban areas.

In a particular frequency band, the wave-media interactions over distributed areas are generally studied using the polarimetric covariance matrix (called also coherency when vectorizing in the Pauli basis). Its use is directly linked to the basic Sinclair model, as this descriptor does not depend on the wave propagation term common to all polarimetric channels. However, among the difficulties encountered when using POLSAR imagery, one important feature is the presence of speckle. Occurring in all types of coherent imagery, the speckle is due to the random interference of the waves scattered by the elementary targets belonging to one resolution cell [2]. In general, POLSAR data are locally modelled by the multivariate, zero mean, circular Gaussian probability density function, which is completely determined by the covariance matrix [3]. With Gaussian clutter, the covariance Maximum Likelihood estimator is the Sample Covariance Matrix (SCM).

The recently launched POLSAR systems are now capable of producing high quality images of the Earth's surface with meter resolution. The decrease of the resolution cell offers the opportunity to observe much thinner spatial features than the decametric resolution of the up-to-now available SAR images. Recent studies [4] show that the higher scene heterogeneity leads to non-Gaussian clutter modelling, especially for urban areas. One commonly used fully polarimetric non-Gaussian clutter model is the product model [5]: the spatial non-homogeneity is incorporated by modelling the clutter as the product between the square root of a scalar random variable (texture) and an independent, zero mean, complex circular Gaussian random vector (speckle). If the texture random variable is supposed to be a Gamma spatial distributed intensity, the product model is equivalent to the well-known  $\mathcal{K}$ -

distributed clutter model [6]. When using the product model, one can notice that the speckle presents a dual nature depending on the involved polarimetric descriptor:

- intensity texture descriptor: speckle can be considered as a nuisance parameter as the Gaussian kernel induces undesired spatial variations over the areas homogeneous in terms of texture,
- covariance matrix descriptor: speckle represents the useful signal as the covariance matrix is computed using the Gaussian kernel, while the texture appears as nuisance.

The POLSAR information allows the discrimination of different scattering mechanisms. In [7], Cloude and Pottier introduced the target entropy and the entropy-alpha-anisotropy ( $H/\alpha/A$ ) model by assigning to each eigenvector the corresponding coherent single scattering mechanism. Based on this decomposition, unsupervised classification for land applications was performed by an iterative algorithm based on complex Wishart density function [8].

The objective of this paper is to present a new coherency estimation technique [9] based on the Spherically Invariant Random Vectors (SIRV) model [10], and to analyze the consequences that this model has on the conventional POLSAR processing chain. The paper is organized as follows. Sect. 2 is dedicated to the presentation of the proposed estimation scheme. The heterogeneity of polarimetric textured scenes is taken into account by coupling the ML normalized coherency estimator with adaptive neighborhoods driven on the scalar ML span estimators. A new ML distance measure is presented in Sect. 3 introduced for classifying normalized coherency matrices under the SIRV model. In Sect. 4, the results obtained using the proposed approach are presented and compared to those given by the Gaussian ML estimator. Results of  $H/\alpha/A$  decomposition, followed by unsupervised POLSAR classification allow to discuss the use of the normalized coherency and the span as two separate descriptors of POLSAR data sets. Eventually, in Sect. 5, some conclusions and perspectives are presented.

## 2. ML PARAMETER ESTIMATION

Spherically Invariant Random Vectors (SIRV) and their applications to estimation and detection in communication theory were firstly introduced by Kung Yao [10]. The SIRV is a class of non-homogeneous Gaussian processes with random variance. The complex  $m$ -dimensional measurement  $\vec{k}$  is defined as the product between the independent complex circular Gaussian vector  $\vec{z}$  (speckle) with zero mean and covariance matrix  $[M] = E\{\vec{z}\vec{z}^\dagger\}$  and the square root of the positive random variable  $\tau$  (representing the texture):

$$\vec{k} = \sqrt{\tau}\vec{z}, \quad (1)$$

It is important to notice that in the SIRV definition, the PDF of the texture random variable is not explicitly specified. As a consequence, SIRVs describe a whole class of stochastic processes defined by Eq. 1. This class includes the conventional clutter models having Gaussian,  $\mathcal{K}$ -distributed, Chi, Rayleigh, Weibull or Rician PDFs [11].

When using the product model, an identification problem can be pointed out: the SIRV model is uniquely defined with respect to the covariance matrix parameter up to a multiplicative constant. Let  $[M_1]$  and  $[M_2]$  be two covariance matrices such that  $[M_1] = \kappa \cdot [M_2]$ , ( $\forall \kappa \in \mathbb{R}_+^*$ ). Notice that the two sets of parameters defined as  $\{\tau_1, [M_1]\}$  and  $\{\tau_2 = \frac{\tau_1}{\sqrt{\kappa}}, [M_2]\}$  describe the same SIRV. For solving this identification problem, the covariance matrix has to be normalized. In the following the covariance matrix  $[M]$  is normalized such that  $\text{Tr}\{[M]\} = m$ , with  $m$  the dimension of the target vector. One important consequence of the imposed normalization condition is that the resulting normalized polarimetric coherency matrix (NC) reveals information concerning the polarimetric diversity only: the total power information is transferred into the texture random variable.

Let now  $p(\tau)$  be the texture PDF associated to the SIRV model. The Spherically Invariant Random Process (SIRP) corresponding to Eq. 1 has the following PDF [12]:

$$p_m(\vec{k}) = \int_0^{+\infty} \frac{1}{(\pi\tau)^m \det\{[M]\}} \exp\left(-\frac{\vec{k}^\dagger [M]^{-1} \vec{k}}{\tau}\right) p(\tau) d\tau. \quad (2)$$

Given a SIRP, this process is wide-sense stationary if and only if both the texture random variable and the speckle random vector are wide-sense stationary. As the speckle is a zero mean complex Gaussian vector, the latter means that the statistical samples  $\vec{k}_i$  used in the estimation process must have the same theoretical covariance matrix  $[M]$ . This condition is called "matrix stationarity".

However, as the results presented in this section can be applied whatever the texture PDF ( $\forall p(\tau)$ ), the previous properties can be reformulated using the SIRV class of stochastic processes. Given a "matrix stationary" stochastic process, this process is "SIRV homogeneous" if and only if the texture random variable is "texture homogeneous". Where "texture homogeneous" means that it is possible to define a texture PDF ( $\exists p(\tau)$ ) such that the stochastic process can be described by the product model from Eq. 1.

We illustrate these properties using four local populations which often occur in practical POLSAR applications:

- One zero mean Gaussian process with covariance matrix  $[M]$ :  $\mathcal{N}(0, [M])$ . Being a "Gaussian sta-

tionary<sup>1</sup>” process, it is also ”SIRP stationary” and ”SIRV homogeneous”. This model is widely used for POLSAR data analysis [13].

- Two adjacent Gaussian processes with different covariance matrix:  $\mathcal{N} = \{\mathcal{N}^{(1)}(0, [M]_1), \mathcal{N}^{(2)}(0, [M]_2)\}$ . The Gaussian mixture  $\mathcal{N}$  is neither ”SIRP stationary” nor ”SIRV homogeneous” as the ”matrix stationarity” condition is not respected. Generally, such cases are treated by employing adaptive estimation schemes [14], [15] in order to approximate the local ”Gaussian stationarity” condition.
- One  $\mathcal{K}$ -distributed process [16] with Gamma distributed texture  $p_G(\tau; \bar{\tau}, \nu)$  and covariance matrix  $[M]: F_{\mathcal{K}}\{p_G(\tau; \bar{\tau}, \nu), [M]\}$ . This process is ”SIRP stationary” as it is ” $\mathcal{K}$  stationary<sup>2</sup>” but obviously it is not ”Gaussian stationary”.
- Two adjacent  $\mathcal{K}$ -distributed processes with two different Gamma texture PDF  $p_G^{(1)}(\tau; \bar{\tau}_1, \nu_1)$ ,  $p_G^{(2)}(\tau; \bar{\tau}_2, \nu_2)$  and the same covariance matrix  $[M]: F_{\mathcal{K}} = \{F_{\mathcal{K}}^{(1)}, F_{\mathcal{K}}^{(2)}\}$ . The  $\mathcal{K}$ -distributed processes  $F_{\mathcal{K}}^{(1)}\{p_G^{(1)}(\tau; \bar{\tau}_1, \nu_1), [M]\}$  and  $F_{\mathcal{K}}^{(2)}\{p_G^{(2)}(\tau; \bar{\tau}_2, \nu_2), [M]\}$  are ”SIRP stationary” and ” $\mathcal{K}$  stationary”, but the mixture  $F_{\mathcal{K}}$  is not ” $\mathcal{K}$  stationary”. Despite this, the process  $F_{\mathcal{K}}$  is ”SIRV homogeneous” as it is possible to define a texture PDF which models the Gamma mixture. As a consequence, the results presented in this section can still be applied in this case.

In conclusion, the two properties to be verified in order to apply the SIRV model are the ”matrix stationarity” and the ”texture homogeneity”. Moreover, the latter considerably relaxes the ”texture stationarity” condition required when using explicit texture models such as the Gamma or the Fisher PDF.

## 2.1. Normalized Covariance Matrix

In Eqs. 1 and 2, the normalized covariance matrix is an unknown parameter which can be estimated from ML theory. In [12], Gini et al. derived the exact ML estimate  $[\hat{M}]$  of the normalized covariance matrix when  $\tau_i$  are assumed to be unknown deterministic quantities. For  $N$  independent and identically distributed (i.i.d.) data, the likelihood function to maximize with respect to  $[M]$

and  $\tau_i$ , is given by:

$$L_{\vec{k}}(\vec{k}_1, \dots, \vec{k}_N; [M], \tau_1, \dots, \tau_N) = \frac{1}{\pi^{mN} \det\{[M]\}^N} \times \prod_{i=1}^N \frac{1}{\tau_i^m} \exp\left(-\frac{\vec{k}_i^\dagger [M]^{-1} \vec{k}_i}{\tau_i}\right). \quad (3)$$

Maximizing  $L_{\vec{k}}(\vec{k}_1, \dots, \vec{k}_N; [M], \tau_1, \dots, \tau_N)$  with respect to  $\tau_i$  yields the texture ML estimator

$$\hat{\tau}_i = \frac{\vec{k}_i^\dagger [M]^{-1} \vec{k}_i}{m}. \quad (4)$$

Replacing  $\tau_i$  in Eq. 3 by their ML estimates the generalized likelihood is obtained as:

$$L'_{\vec{k}}(\vec{k}_1, \dots, \vec{k}_N; [M]) = \frac{1}{\pi^{mN} \det\{[M]\}^N} \times \prod_{i=1}^N \frac{m^m \exp(-m)}{(\vec{k}_i^\dagger [M]^{-1} \vec{k}_i)^m}. \quad (5)$$

The ML estimator of the normalized covariance matrix in the deterministic texture case is obtained by cancelling the gradient of  $L'_{\vec{k}}$  with respect to  $[M]$  as the solution of the following recursive equation:

$$[\hat{M}]_{FP} = f([\hat{M}]_{FP}) = \frac{m}{N} \sum_{i=1}^N \frac{\vec{k}_i \vec{k}_i^\dagger}{\vec{k}_i^\dagger [\hat{M}]_{FP}^{-1} \vec{k}_i}. \quad (6)$$

This approach has been used in [17] by Conte et al. to derive a recursive algorithm for estimating the matrix  $[M]$ . This algorithm consists in computing the Fixed Point of  $f$  using the sequence  $([M]_i)_{i \geq 0}$  defined by:

$$[M]_{i+1} = f([M]_i). \quad (7)$$

It has been shown in [12] and [17] that the estimation scheme from Eq. 6, developed under the deterministic texture case, yields also an approximate ML estimator under stochastic texture hypothesis. This study has been completed by the work of Pascal et al. [9], [18], which recently established the existence and the uniqueness, up to a scalar factor, of the Fixed Point estimator of the normalized covariance matrix, as well as the convergence of the recursive algorithm whatever the initialization. The algorithm can therefore be initialized with the identity matrix  $[M]_0 = [I_m]$ .

We propose to apply these results in estimating normalized coherency matrices for high resolution POLSAR data. The main advantage of this approach is that the local ”scene heterogeneity” can be taken into account without any ”a priori” hypothesis regarding the texture random variable  $\tau$  (Eq. 7 does not depend on  $\tau$ ). The obtained Fixed Point is the approximate ML estimate under the stochastic  $\tau$  assumption and the exact ML under deterministic  $\tau$  assumption. Moreover, the normalized polarimetric coherency matrix estimated using the Fixed Point method is unbiased and asymptotically Gaussian distributed [9], [18].

Note that the multivariate Gaussian distribution is a member of the SIRV class. Let us assume  $N$  i.i.d. realizations

<sup>1</sup>A ”Gaussian stationary” process is a stochastic process whose Gaussian PDF does not change when shifted in time or space.

<sup>2</sup>A ” $\mathcal{K}$  stationary” process is a stochastic process whose  $\mathcal{K}$  PDF does not change when shifted in time or space.

of the target vector  $\vec{k}$ . The SCM is the ML estimator of  $[T]$  in Gaussian clutter, but not in clutter described by the product model [19]. In the specific case of completely correlated texture ( $\tau = \tau_i, \forall i \in \{1, \dots, N\}$ ), Richmond proved that SCM is again the exact ML estimator of  $[M]$  provided the M-normalization is respected [20]. In fact, the completely correlated  $\tau$  case is equivalent to the Gaussian model for a given realization of data across all resolution cells [12]. Consequently, it is possible to define the Sample Covariance matrix Normalized (SCN) as:

$$[\widehat{M}]_{SCN} = m \frac{[\widehat{T}]_{SCM}}{\text{Tr}\{[\widehat{T}]_{SCM}\}} \quad (8)$$

In this paper, we propose to use the SCN for assessing the performance of the FP estimator.

## 2.2. Span

Note also that the texture estimator from Eq. 4 can be directly linked to the total scattered power (span). By estimating the normalized coherency as the Fixed Point solution of Eq. 6, the derived NC is independent of the total power and it contains polarimetric information only. Using this matrix, it is possible to compute the SIRV span ML estimator for unknown deterministic  $\tau$  as:

$$\widehat{P}_{PWF} = \vec{k}^\dagger [\widehat{M}]_{FP}^{-1} \vec{k}. \quad (9)$$

One can observe that the span estimator from Eq. 9 has the same form as the Polarimetric Whitening Filter (PWF) introduced by Novak et al. in [21]. The only difference is the use of the NC given by the Fixed Point estimator instead of the conventional Sample Covariance Matrix.

Finally, it is possible to derive an estimate of the conventional polarimetric coherency matrix according to Eq. 1:

$$[\widehat{T}]_{FP} = \frac{\widehat{P}_{PWF}}{m} [\widehat{M}]_{FP}. \quad (10)$$

## 3. OPTIMAL GLRT DISTANCE MEASURES

When the POLSAR data are modelled by a stochastic process with a known PDF, it is possible to derive optimal ML distance measures (e.g. the Wishart distance for Gaussian processes). For this purpose, we propose the following general binary hypothesis test for a given class  $\omega$ :

$$\begin{cases} H_0 : [C] = [C]_\omega \\ H_1 : [C] \neq [C]_\omega \end{cases} \quad (11)$$

According to the Neyman-Pearson Lemma, the LRT (Likelihood Ratio Test) provides the most powerful test [22]:

$$\Lambda = \frac{p_m(\vec{k}_1, \dots, \vec{k}_N / H_1)}{p_m(\vec{k}_1, \dots, \vec{k}_N / H_0)}. \quad (12)$$

After briefly introducing the Wishart distance as the result of GLRT (Generalized LRT) maximization, the following section is dedicated to deriving the optimal ML distance measure associated to the SIRV model with deterministic unknown texture.

### 3.1. Gaussian clutter

For Gaussian clutter, the binary hypothesis test from Eq. 11 becomes:

$$\begin{cases} H_0 : [T] = [T]_\omega & \Leftrightarrow \vec{k} \sim \mathcal{N}(0, [T]) \\ H_1 : [T] \neq [T]_\omega & \Leftrightarrow \vec{k} \sim \mathcal{N}(0, [T]_\omega) \end{cases} \quad (13)$$

By considering  $N$  i.i.d. samples, the Likelihood Ratio Test (LRT) for the Gaussian model is:

$$\Lambda_G = \frac{\prod_{n=1}^N \frac{\exp\left\{-\vec{k}_n^\dagger [T]_\omega^{-1} \vec{k}_n\right\}}{\pi^m \det\{[T]_\omega\}}}{\prod_{n=1}^N \frac{\exp\left\{-\vec{k}_n^\dagger [T]^{-1} \vec{k}_n\right\}}{\pi^m \det\{[T]\}}} \quad (14)$$

Taking the natural logarithm and maximizing the LRT from Eq. 14 is equivalent to minimizing the following distance with respect to  $[T]$ :

$$D_G = \ln \frac{\det\{[T]_\omega\}}{\det\{[T]\}} + \frac{1}{N} \sum_{n=1}^N \vec{k}_n^\dagger ([T]_\omega^{-1} - [T]^{-1}) \vec{k}_n \quad (15)$$

By replacing the pixel coherency matrix  $[T]$  with the ML estimate  $[\widehat{T}]_{SCM}$ , the LRT from Eq. 14 becomes the Generalized LRT and the associated distance measure is the conventional Wishart distance:

$$\begin{aligned} D_W &= \ln \frac{\det\{[T]_\omega\}}{\det\{[\widehat{T}]_{SCM}\}} + \frac{1}{N} \sum_{n=1}^N \vec{k}_n^\dagger [T]_\omega^{-1} \vec{k}_n \\ &= \ln \frac{\det\{[T]_\omega\}}{\det\{[\widehat{T}]_{SCM}\}} + \text{Tr}\left\{[T]_\omega^{-1} [\widehat{T}]_{SCM}\right\} \end{aligned} \quad (16)$$

This distance has been widely used for supervised and unsupervised POLSAR data clustering [8], [23].

### 3.2. SIRV clutter

For the SIRV model, one can rewrite the hypothesis test as:

$$\begin{cases} H_0 : [M] = [M]_\omega & \Leftrightarrow \vec{k} = \sqrt{\tau} \vec{z}, \vec{z} \sim \mathcal{N}(0, [M]) \\ H_1 : [M] \neq [M]_\omega & \Leftrightarrow \vec{k} = \sqrt{\tau} \vec{z}, \vec{z} \sim \mathcal{N}(0, [M]_\omega) \end{cases}$$

where  $\tau$  is the unknown deterministic texture.

For a given class  $[M]_\omega$ , the LRT with respect to the texture  $\tau$  and the normalized coherency matrix  $[M]$  is given

by:

$$\Lambda_{SIRV} = \frac{\prod_{n=1}^N \frac{1}{\pi^m \tau_n^m \det\{[M]_\omega\}} \exp \left\{ -\frac{\vec{k}_n^\dagger [M]_\omega^{-1} \vec{k}_n}{\tau_n} \right\}}{\prod_{n=1}^N \frac{1}{\pi^m \tau_n^m \det\{[M]\}} \exp \left\{ -\frac{\vec{k}_n^\dagger [M]^{-1} \vec{k}_n}{\tau_n} \right\}} \quad (17)$$

By taking the natural logarithm, one obtains:

$$\begin{aligned} \ln(\Lambda_{SIRV}) &= -N \ln \frac{\det\{[M]_\omega\}}{\det\{[M]\}} - \\ &- \sum_{n=1}^N \frac{\vec{k}_n^\dagger ([M]_\omega^{-1} - [M]^{-1}) \vec{k}_n}{\tau_n}. \end{aligned} \quad (18)$$

Now, since the  $\tau_n$ 's and  $[M]$  are unknown, they are replaced by their ML estimates from Eq. 4 and Eq. 6. The resulting Generalized Likelihood Ratio Test  $\Lambda'_{SIRV}$  is given by:

$$\begin{aligned} \ln(\Lambda'_{SIRV}) &= -N \ln \frac{\det\{[M]_\omega\}}{\det\{[\widehat{M}]_{FP}\}} - \\ &- m \sum_{n=1}^N \frac{\vec{k}_n^\dagger [M]_\omega^{-1} \vec{k}_n}{\vec{k}_n^\dagger [\widehat{M}]_{FP}^{-1} \vec{k}_n} + Nm. \end{aligned} \quad (19)$$

Maximizing the GLRT over all classes is equivalent to minimizing the following SIRV distance:

$$D_{SIRV} = \ln \frac{\det\{[M]_\omega\}}{\det\{[\widehat{M}]_{FP}\}} + \frac{m}{N} \sum_{n=1}^N \frac{\vec{k}_n^\dagger [M]_\omega^{-1} \vec{k}_n}{\vec{k}_n^\dagger [\widehat{M}]_{FP}^{-1} \vec{k}_n}. \quad (20)$$

In this paper, the distance measure from Eq. 20 is used as a dissimilarity measure in the conventional K-means clustering for POLSAR data. The full description of the K-means algorithm can be found in [8].

#### 4. RESULTS AND DISCUSSION

The POLSAR data (Fig. 1) set was acquired by the ONERA RAMSES system over Toulouse, France with a mean incidence angle of  $50^\circ$ . It represents a fully polarimetric (monostatic mode) X-band acquisition with a spatial resolution of approximately 50 cm in range and azimuth.

Three different estimation techniques are analyzed: the Sample Covariance matrix Normalized coupled with the  $7 \times 7$  Boxcar Neighborhood (BN-SCN) and the Fixed Point estimator coupled either with the  $7 \times 7$  Boxcar Neighborhood (BN-FP) or with the Span-Driven-Adaptive-Neighborhood (SDAN-FP) [24]. In all three cases, the corresponding span image is estimated using the LLMMSE estimator as presented in [24]. The parameters used for the SDAN algorithm are  $L_{eq} = 3$  and  $N_{max} = 50$ .

The effectiveness of the Fixed Point estimator in compound Gaussian clutter can be observed in Fig. 2. While the BN-SCN normalized coherency [Fig. 2-(a)] presents

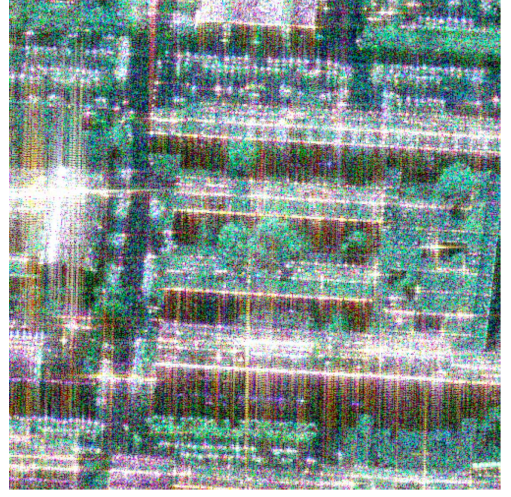


Figure 1. RAMSES POLSAR data, X-band ( $501 \times 501$  pixels). Amplitude color composition of the target vector elements  $k_1$ - $k_3$ - $k_2$ .

a "patchy" appearance, the BN-FP estimation [Fig. 2-(b)] provides better visual homogeneity within each quadrant. This shows that the FP estimate of the covariance matrix does not depend on the texture PDF.

One key issue to be discussed is whether the normalized coherency matrix (NC) and the span should be aggregated in the final estimation step or not. Most of the existing processing chains use the conventional coherency matrix for representing POLSAR data for unsupervised land cover classification [8], [23], and for target detection applications [16]. Due to the SIRV model identification problem, the complete description of the POLSAR data set is achieved by estimating the span and the normalized coherency independently. The NC describes the polarimetric diversity, while the span indicates the total received power. Moreover, the Fixed Point estimation of the normalized coherence does not depend on the span information. Given these facts, we propose to investigate this problem in the framework of unsupervised POLSAR classification. The classification scheme discussed in the following is the standard Wishart  $H/\alpha$  segmentation [8]. For segmenting the normalized coherency, we have modified the Wishart  $H/\alpha$  algorithm by replacing the Wishart distance with the SIRV ML distance discussed in Sect. 3.2. For comparison, we have also used the scalar Gamma K-means classification with  $H/\alpha$  initialization. The corresponding ML distance measure is obtained using the GLRT with the Gamma PDF.

Fig. 3 illustrates the POLSAR unsupervised classification results using three descriptors estimated by SDAN-FP: span [Fig. 3-(a)], normalized coherency [Fig. 3-(c)] and coherency [Fig. 3-(e)]. The selected scene is composed of both Gaussian (streets) and non-Gaussian (urban) areas. Fig. 3-(f) presents the standard classification map obtained using the SDAN-FP coherency matrix. When compared to the scalar unsupervised classification map [Fig. 3-(b)] obtained using span only, one can observe



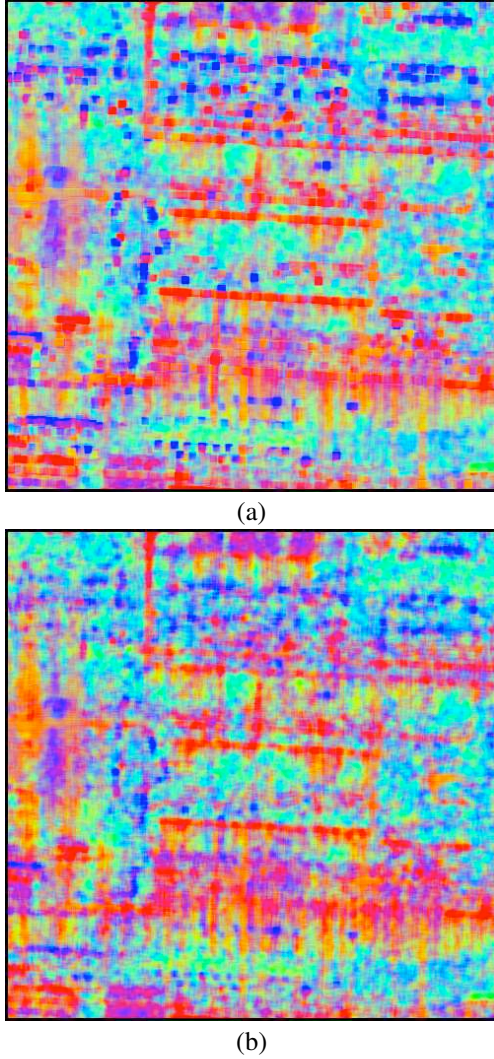


Figure 2. RAMSES POLSAR data, X-band ( $501 \times 501$  pixels). Color composition of the normalized coherency diagonal elements  $[M]_{11}$ - $[M]_{33}$ - $[M]_{22}$  estimated within the  $7 \times 7$  boxcar neighborhood using: (a) the Sample Covariance matrix Normalized estimator BN-SCN and (b) the Fixed Point estimator BN-FP.

the high degree of similarity between them. This leads to the following conclusion: the Wishart  $H/\alpha$  classification is mainly influenced by the information contained in the span image. Regarding the polarimetric information, Fig. 3-(d) presents the classification map computed using the normalized coherency matrix and the associated SIRV distance. The visual assessment of Fig. 3-(d) and Fig. 3-(f) reveals that a significant part of the polarimetric information is lost when using the standard coherency matrix.

Finally, the joint analysis of the span and the normalized coherency (NC) presents several advantages with respect to the coherency matrix descriptor: separation between the total received power and the polarimetric information, estimation of the NC independently of the span and the existence of the SIRV distance measure for unsuper-

vised ML classification of normalized coherencies. However, the span-NC description of POLSAR images raises new problems which still remain under investigation. The first issue concerns the use of span for testing the "matrix stationarity" condition for the normalized coherency estimation. This test is currently used for POLSAR data speckle filtering and it is founded on the basic principle that changes within the polarimetric signature are revealed by changes in the total received power. Consequently, one may envisage other estimation schemes dedicated to the SIRV model with stochastic texture by considering external estimators of "matrix stationarity". The second important remark concerns the Wishart unsupervised classification scheme. Although all statistical requirements employed for unsupervised classification are met, the polarimetric information is quite difficult to extract using the K-means clustering. As it can be noticed in Fig. 3-(c),(d), the polarimetric signatures are strongly mixed and the class boundaries are smoothed within high resolution POLSAR images (even for highly heterogeneous target areas). Therefore, other clustering strategies [25] should be better suited to capture the spatial distribution of different polarimetric signatures.

## 5. CONCLUSION

This paper presented a new estimation scheme for deriving normalized coherency matrices and the resulting estimated span with high resolution POLSAR images. The proposed approach couples nonlinear ML estimators with span driven adaptive neighborhoods for taking the local scene heterogeneity into account.

The heterogeneous clutter in POLSAR data was described by the SIRV model. Two estimators were introduced for describing the POLSAR data set: the Fixed Point estimator of normalized coherency matrix and the corresponding LLMMSE span. The Fixed Point estimation is independent on the span PDF and represents an approximate ML estimator for a large class of stochastic processes obeying the SIRV model. Moreover, the derived normalized coherency is asymptotically Gaussian distributed.

For SIRV clutter, a new ML distance measure was introduced for unsupervised POLSAR classification. This distance was used in conventional K-means clustering initialized by the  $H/\alpha$  polarimetric decomposition. Other extensions of the existing unsupervised or supervised POLSAR clustering methods (e.g. Bayes ML or fuzzy K-means) can be derived by replacing the conventional Wishart distance with the proposed SIRV distance.

## ACKNOWLEDGMENTS

This work was supported by the French Space Agency CNES and by the French ANR program EFIDIR.



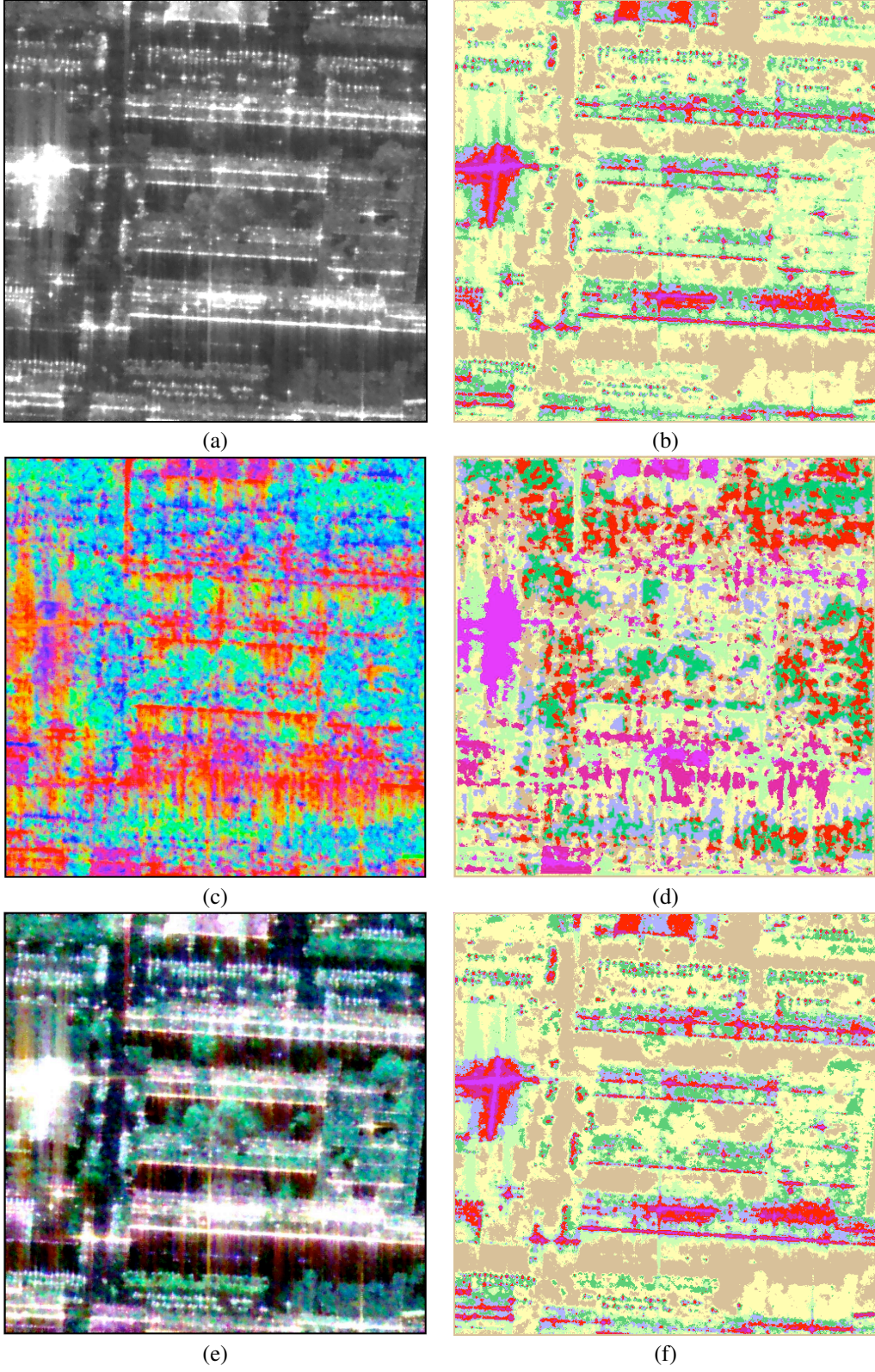


Figure 3. RAMSES POLSAR data, X-band ( $501 \times 501$  pixels), Fixed Point normalized coherency estimator within the SDAN neighborhood SDAN-FP. (a) LLMMSE span and (b) unsupervised scalar Gamma span segmentation. (c) Color composition of the normalized coherency diagonal elements  $[M]_{11}$ - $[M]_{33}$ - $[M]_{22}$  and (d) unsupervised  $H/\alpha$  SIRV normalized coherency segmentation. (e) Color composition of the diagonal elements of the diagonal elements  $[T]_{11}$ - $[T]_{33}$ - $[T]_{22}$  and (f) unsupervised  $H/\alpha$  Wishart coherency segmentation.

## REFERENCES

- [1] W. M. Boerner. Basic concepts of radar polarimetry and its applications to target discrimination, classification, imaging, and identification. Technical Report EMID-CL-82-05-18-0, Communications Laboratory, University of Illinois, Chicago, USA, 1982.
- [2] J. W. Goodman. Some fundamental properties of speckle. *J. Opt. Soc. Amer.*, 53(11):1145–1149, 1976.
- [3] C. Lopez-Martinez and X. Fabregas. Polarimetric SAR speckle noise model. *IEEE Transactions on Geoscience and Remote Sensing*, 44(10):2232–2242, 2003.
- [4] M. S. Greco and F. Gini. Statistical analysis of high-resolution SAR ground clutter data. *IEEE Transactions on Geoscience and Remote Sensing*, 45(3):566–575, 2007.
- [5] F. T. Ulaby, F. Kouyate, B. Brisco, and T. H. L. Williams. Textural information in SAR images. *IEEE Transactions on Geoscience and Remote Sensing*, GE-24(2):235–245, 1986.
- [6] J. K. Jao. Amplitude distribution of composite terrain radar clutter and the K-distribution. *IEEE Transactions on Antennas and Propagation*, AP-32(10):1049–1062, 1984.
- [7] S. R. Cloude and E. Pottier. An entropy based classification scheme for land applications of polarimetric SAR. *IEEE Transactions on Geoscience and Remote Sensing*, 35(1):68–78, 1997.
- [8] J. S. Lee, M. R. Grunes, T. L. Ainsworth, D. Li-Jen, D. L. Schuler, and S. R. Cloude. Unsupervised classification using polarimetric decomposition and the complex Wishart classifier. *IEEE Transactions on Geoscience and Remote Sensing*, 37(5):2249–2258, 1999.
- [9] F. Pascal, Y. Chitour, J. P. Ovarlez, P. Forster, and P. Larzabal. Covariance structure maximum-likelihood estimates in compound Gaussian noise: existence and algorithm analysis. *IEEE Transactions on Signal Processing*, 56(1):34–48, 2008.
- [10] K. Yao. A representation theorem and its applications to spherically-invariant random processes. *IEEE Transactions on Information Theory*, 19(5):600–608, 1973.
- [11] M. Rangaswamy, D. Weiner, and A. Ozturk. Computer generation of correlated non-Gaussian radar clutter. *IEEE Transactions on Aerospace and Electronic Systems*, 31(1):106–116, 1995.
- [12] F. Gini and M. V. Greco. Covariance matrix estimation for CFAR detection in correlated heavy tailed clutter. *Signal Processing*, 82(12):1847–1859, 2002.
- [13] N. R. Goodman. Statistical analysis based on a certain multivariate complex gaussian distribution (an introduction). *Annals of Mathematical Statistics*, 34(1):152–177, 1963.
- [14] J. S. Lee, M. R. Grunes, and G. DeGrandi. Polarimetric SAR speckle filtering and its impact on terrain classification. *IEEE Transactions on Geoscience and Remote Sensing*, 37(5):2363–2373, 1999.
- [15] G. Vasile, E. Trouvé, J. S. Lee, and V. Buzuloiu. Intensity-Driven-Adaptive-Neighborhood technique for polarimetric and interferometric SAR parameters estimation. *IEEE Transactions on Geoscience and Remote Sensing*, 44(5):1609–1621, 2006.
- [16] L. M. Novak, M. B. Sechtn, and M. J. Cardullo. Studies of target detection algorithms that use polarimetric radar data. *IEEE Transactions on Aerospace and Electronic Systems*, 25(2):150–165, 1989.
- [17] E. Conte, A. DeMaio, and G. Ricci. Recursive estimation of the covariance matrix of a compound-Gaussian process and its application to adaptive CFAR detection. *IEEE Transactions on Image Processing*, 50(8):1908–1915, 2002.
- [18] F. Pascal, P. Forster, J. P. Ovarlez, and P. Larzabal. Performance analysis of covariance matrix estimates in impulsive noise. *IEEE Transactions on Signal Processing*, 56(6):2206–2216, 2008.
- [19] E. J. Kelly. An adaptive detection algorithm. *IEEE Transactions on Aerospace and Electronic Systems*, AES-22(2):115–127, 1986.
- [20] C. D. Richmond. A note on non-Gaussian adaptive array detection and signal parameter estimation. *IEEE Signal Processing Letters*, 3(8):251–252, 1996.
- [21] L. M. Novak and M. C. Burl. Optimal speckle reduction in polarimetric SAR imagery. *IEEE Transactions on Aerospace and Electronic Systems*, 26(2):293–305, 1990.
- [22] E. L. Lehmann. *Testing statistical hypotheses*. John-Wiley&Sons, Springer-Verlag, New York, USA, 2nd edition, 1986.
- [23] P. R. Kersten, J. S. Lee, and T. L. Ainsworth. Unsupervised classification of polarimetric synthetic aperture radar images using fuzzy clustering and EM clustering. *IEEE Transactions on Geoscience and Remote Sensing*, 43(3):519–527, 2005.
- [24] G. Vasile, J. P. Ovarlez, F. Pascal, C. Tison, L. Bombrun, M. Gay, and E. Trouvé. Normalized coherency matrix estimation under the SIRV model. Alpine glacier POLSAR data analysis. In *Proceedings of the IEEE International Geoscience and Remote Sensing Symposium, Boston, USA*, page to appear, 2008.
- [25] J. M. Beaulieu and R. Touzi. Segmentation of textured polarimetric SAR scenes by likelihood approximation. *IEEE Transactions on Geoscience and Remote Sensing*, 42(10):2063–2072, 2004.